

## Electronic structure of ternary random alloys

This article has been downloaded from IOPscience. Please scroll down to see the full text article.

1997 J. Phys.: Condens. Matter 9 6607

(<http://iopscience.iop.org/0953-8984/9/31/013>)

View [the table of contents for this issue](#), or go to the [journal homepage](#) for more

Download details:

IP Address: 171.66.16.207

The article was downloaded on 14/05/2010 at 09:17

Please note that [terms and conditions apply](#).

## Electronic structure of ternary random alloys

Tanusri Saha† and Abhijit Mookerjee‡

S N Bose National Centre for Basic Sciences, JD Block, Sector 3, Salt Lake City,  
Calcutta 700091, India

Received 16 July 1996, in final form 10 March 1997

**Abstract.** We present here a technique for the study of the electronic structure of ternary random alloys. The technique is based on the augmented space recursion introduced earlier by us for binary alloys. The method discussed here is a non-trivial extension of the earlier technique for binary alloys.

### 1. Introduction

Commercial alloys are multiphase systems. In addition to having knowledge about the electronic structure of pure elements and ordered intermetallics one should also possess an understanding of the electronic structure of disordered phases. The majority of electronic structure calculations for disordered alloys deal with binary substitutional alloys, whereas most alloys of practical interest are multi-component (e.g. ternary, quaternary etc), from semiconductor alloys used in devices to brasses and stainless steels. Binary alloy systems provide a first step in the understanding of higher-order alloy systems. The electronic structure calculations of higher-order alloy systems proves the real predictive power of theory and leads to alloy designing. Furthermore, systems like binary magnetic alloys with random moments or vacancies in binary systems can be thought of as special cases of more general higher-order alloy systems.

Calculations on disordered alloys demand, in conjunction with accurate electronic structure description, a reasonable scheme of describing the configuration averaging. To date the most successful of these schemes is the coherent potential approximation (CPA). Ternary generalizations of the CPA based on the tight-binding linearized muffin-tin orbital method (TB-LMTO) have been carried out [1–4]. Despite its success, the CPA, being a single-site approximation, has its own limitations. In particular, for split band alloys, CPA does not work well in the impurity bands. This was noted, for example, by Hüfner *et al* in the Ni minority bands of Cu-rich NiCu and Pd minority bands of Ag-rich PdAg alloys [5]. It does not include correlated scatterings from neighbouring sites, nor can it take into account short-ranged order [10] or off-diagonal disorder arising out of local lattice distortions [11]. The augmented space formalism [6] for configuration averaging provides a systematic way of taking these effects into account. Recently [7] we have coupled this formalism with the recursion method of Haydock *et al* [8] within the framework of the tight-binding linearized muffin-tin orbital basis (TB-LMTO) [9] for study of the electronic structure of disordered

† Present address: Office National d'Etudes et de Recherches Aérospatiales, Laboratoire de Physique des Solides, BP 72 92322 Chatillon Cédex, France. E-mail address: dasgupta@onera.fr

‡ E-mail address: abhijit@bose.ernet.in

binary alloy systems. This method coupled with the orbital peeling method has been shown [12] to provide a reasonable and computationally viable technique for alloy phase stability studies. A generalization of this method to ternary systems will be an interesting and useful extension.

In section 2 we present briefly what augmented space recursion is. In section 3 we apply the method of augmented space recursion for ternary alloy systems within the framework of TB-LMTO formalism. Section 4 is devoted to computational details. In section 5 we present results for some Cu–Ni–Zn, Ag–Pd–Rh and Fe–Cu–Ag ternary alloy systems.

## 2. The augmented space recursion

The augmented space recursion is based on the augmented space formalism (ASF) [6]. ASF provides an exact method of obtaining configuration averaged quantities. The configuration averaging is done by extending the usual *lattice* space  $\mathcal{H}$  to include the configuration space  $\Phi$  of the relevant random Hamiltonian parameters. The scheme to get the configuration averaging of some function  $f(\{n_i\})$  of a set of random variables  $\{n_i\}$  by ASF is described by the *augmented space theorem*:

(i) A random variable  $n_i$  can take  $N$  different values  $n_{i_1}, \dots, n_{i_N}$ , with probabilities  $x_1, \dots, x_N$ . If the probability density  $p_i(n_i)$  has finite moments to all orders, it can be expressed as a continued fraction. Then there exists a self-adjoint operator  $M^{(i)}$  such that its spectral density is  $p_i(n_i)$ .  $M^{(i)}$  is an operator in a space  $\phi^{(i)}$  spanned by the configurations of  $n_i$  and has a tridiagonal representation with the continued fraction coefficients in the diagonal and off-diagonal positions.

(ii) For the set of independent random variables  $\{n_i\}$  one defines a configuration space  $\Phi = \prod^{\otimes} \phi^{(i)}$ . A self-adjoint operator  $\tilde{M}^{(i)}$  is defined in the configuration space as

$$\tilde{M}^{(i)} = I \otimes \dots \otimes M^{(i)} \otimes \dots \otimes I.$$

(iii) The configuration average of any function  $f(\{n_i\})$  of the set of random variables is given by  $\langle v_0 | f(\{\tilde{M}^{(i)}\}) | v_0 \rangle$  where  $|v_0\rangle = \prod^{\otimes} |v_0^i\rangle$  with  $|v_0^i\rangle = \sum_k \sqrt{x_k} |n_{ik}\rangle$  where  $\sum_k x_k = 1$ . It represents the reference of average state against which configuration fluctuations are described.

For electronic structure calculations the quantity of interest is the Green function. The random variables here are the random occupation numbers at each site of the lattice. These depend upon the type of component occupying the site. According to the ASF scheme, based on the Hamiltonian which is a function of random occupation variables defined in a Hilbert space  $\mathcal{H}$ , one defines a nonrandom Hamiltonian  $\tilde{H}$  in the extended augmented space  $\Psi = \mathcal{H} \otimes \Phi$ , which is the same functional of operators  $\{\tilde{M}^{(i)}\}$  as  $H$  was of the random occupation variables  $\{n_i\}$ . The effective Hamiltonian  $\tilde{H}$  contains complete information about the quantum behaviour of the system described in  $\mathcal{H}$  and its statistical behaviour described in  $\Phi$ . The configuration averaged Green function is given by the resolvent of this augmented Hamiltonian  $\tilde{H}$ . Note that this statement is exact and no approximations are involved at this stage.

In a series of recent communications [7–12] we have shown that the most practical and tractable way of implementing the augmented space formalism is to couple it with the recursion method. We perform recursion with the effective Hamiltonian  $\tilde{H}$  defined in the enlarged augmented space to obtain the configuration averaged Green function. The starting state of augmented space recursion (ASR) is chosen to be  $|\xi\rangle = |R, L, v_0\rangle$ :  $R$  labels the site in which the projected density of state has to be found,  $L$  is a composite angular

momentum index and  $\nu_0$  denotes the average state introduced earlier. The subsequent states in augmented space are generated by the recursion process

$$B_{n+1}|\xi_{n+1}\rangle = (\tilde{H} - A_n)|\xi_n\rangle + B_n|\xi_{n-1}\rangle$$

with

$$B_0 = 1 \quad B_n = \langle \xi | \tilde{H} | \xi_{n+1} \rangle \quad A_n = \langle \xi_n | \tilde{H} | \xi_n \rangle.$$

Recursion is carried out up to a suitable number of steps. The recursion coefficients  $A_n$  and  $B_n$  form the continued fraction expansion coefficients of averaged Green function  $\langle G \rangle$ . Finally the continued fraction is appended with a terminator to simulate the asymptotic part and maintain the essential herglotz analytic properties of the Green function.

### 3. ASR for ternary alloys

We employ the augmented space recursion within the framework of TB-LMTO introduced by Andersen and Jepsen [9] for a first-principles determination of the configuration averaged Green function of disordered ternary alloys. We start from the most localized tight-binding Hamiltonian derived systematically from LMTO-ASA theory and generalized to random ternary alloys as

$$H_{iL,jL'}^\beta = (\tilde{C}_{iL}\delta_{iL}\delta_{jL'})\underline{P}_{iL} + (\tilde{\Delta}_{iL}^{1/2}S_{iL,jL'}^\beta)\Delta_{jL'}^{1/2}T_{iL,jL'}$$

with

$$\begin{aligned} \tilde{C}_{iL} &= C_L^B + \frac{1}{2}(C_L^A - C_L^C)n_i + \frac{1}{2}(C_L^A + C_L^C - 2C_L^B)n_i^2 \\ \tilde{\Delta}_{iL} &= \Delta_L^B + \frac{1}{2}(\Delta_L^A - \Delta_L^C)n_i + \frac{1}{2}(\Delta_L^A + \Delta_L^C - 2\Delta_L^B)n_i^2. \end{aligned}$$

Here  $i, j$  denote the lattice sites and  $L(= \ell, m)$  are the orbital indices ( $\ell \leq 2$ ).  $C_L^A, C_L^B, C_L^C, \Delta_L^A, \Delta_L^B$  and  $\Delta_L^C$  are the potential parameters of the constituents A, B and C of the alloy. The occupation variable  $n_i$  characterizes the ternary random occupation which can take value 1, 0 or  $-1$  according to whether the site labelled by  $i$  is occupied by constituents A, B or C. The screened or tight-binding structure factor  $S^\beta$  contains all the information on lattice geometry and it is expressed in terms of conventional structure factor  $S^0$  and the screening parameter  $\beta$  as

$$S^\beta = S^0(1 - \beta S^\beta).$$

For a random ternary alloy with constituent concentrations  $x_A, x_B$  and  $x_C$  the probability density of occupation variable  $n_i$  is

$$p(n_i) = x_A\delta(n_i - 1) + x_B\delta(n_i) + x_C\delta(n_i + 1) \quad (1)$$

which can be rewritten as

$$(-1/\pi) \operatorname{Im} \left\{ \frac{x_A}{n_i^+ - 1} + \frac{x_B}{n_i^+} + \frac{x_C}{n_i^+ + 1} \right\}.$$

According to the ASF scheme, we begin by finding a continued fraction expansion of the expression in curly brackets to obtain a representation of the self-adjoint matrix  $M^{(i)}$ .

As shown in an earlier communication [13] the continued fraction expansion coefficients are given by

$$\begin{aligned}
 \alpha_1 &= (x_A - x_C) \\
 \beta_1^2 &= (x_A + x_C) - (x_A - x_C)^2 \\
 \alpha_2 &= \frac{(x_A - x_C)x_B}{x_A + x_C - (x_A - x_C)^2} - x_A + x_C \\
 \beta_2^2 &= x_B + \frac{(x_A - x_C)x_B}{x_A + x_C - (x_A - x_C)^2} \left\{ x_A - x_C - \frac{(x_A - x_C)x_B}{x_A + x_C - (x_A - x_C)^2} \right\} \\
 \alpha_3 &= \frac{(x_A - x_C)x_B}{-x_A - x_C + (x_A - x_C)^2}
 \end{aligned} \tag{2}$$

where

$$p_{n_i} = (-1/\pi) \operatorname{Im} \frac{1}{n_i^+ - \alpha_1 - \beta_1^2/[n_i^+ - \alpha_2 - \beta_2^2/(n_i^+ - \alpha_3)]}.$$

The corresponding representation of the operator  $M^{(i)}$  is a  $3 \times 3$  matrix. In operator representation

$$\begin{aligned}
 M^{(i)} &= \sum_{kk'} \Gamma_{kk'} \mathcal{T}_{kk'} \\
 N^{(i)} &= \sum_{kk'} \mathcal{S}_{kk'} \mathcal{T}_{kk'}.
 \end{aligned} \tag{3}$$

$N^{(i)} = M^{(i)} M^{(i)}$ . Here  $\mathcal{T}_{kk'}$  is the projection operator  $P_k$  if  $k = k'$  or the transfer operator  $T_{kk'}$  if  $k \neq k'$  and

$$\Gamma = \begin{pmatrix} \alpha_1 & \beta_1 & 0 \\ \beta_1 & \alpha_2 & \beta_2 \\ 0 & \beta_2 & \alpha_3 \end{pmatrix} \tag{4}$$

$$\mathcal{S} = \begin{pmatrix} \alpha_1^2 + \beta_1^2 + \beta_2^2 & \beta_1(\alpha_1 + \alpha_2) & \beta_2(\alpha_1 + \alpha_3) \\ \beta_1(\alpha_1 + \alpha_2) & \alpha_2^2 + \beta_1^2 & \beta_1\beta_2 \\ \beta_2(\alpha_1 + \alpha_3) & \beta_1\beta_2 & \alpha_3^2 + \beta_2^2 \end{pmatrix}. \tag{5}$$

Considering the TB-LMTO Hamiltonian for the random ternary alloy and defining

$$\begin{aligned}
 X_{1L} &= X_L^B \\
 X_{2L} &= \frac{1}{2}(X_L^A - X_L^C) \\
 X_{3L} &= \frac{1}{2}(X_L^A + X_L^C - 2x_L^B)
 \end{aligned}$$

(where  $X_L$  is either  $C_L$  of  $\Delta_L^{1/2}$ ), the augmented Hamiltonian defined in the augmented space is given by

$$\tilde{H} = \sum_i \hat{C}_{iL} \otimes \underline{P}_{iL} + \sum_{ij} \hat{\Delta}_{iL}^{1/2} \otimes S_{iL,jL} \mathcal{T}_{iL,jL} \otimes \hat{\Delta}_{jL}^{1/2} \tag{6}$$

with

$$\hat{X}_{iL} = X_{1L} + X_{2L} M^{(i)} + X_{3L} N^{(i)}.$$

Defining  $(\Delta_L^x)^{1/2} S_{iL,jL'} (\Delta_{L'}^y)^{1/2} - h_{iL,jL'}^{xy}$  with  $x, y = A, B, C$  and collecting all terms together we obtain

$$\begin{aligned} \tilde{H} = & \hat{C}_{iL} I \otimes I + \sum_{iL,jL'} h_{iL,jL'}^{BB} I \otimes T_{iL,jL'} + \sum_{iL} \sum_{k \neq k'} E_{kk'}^{iL} \mathcal{T}_{kk'}^{(i)} \otimes P_{iL} + \dots \\ & \dots + \sum_{iL,jL'} \sum_{kk'} \{ (h_{iL,jL'}^{BA} \Gamma_{kk'} + h_{iL,jL'}^{BC} \mathcal{S}_{kk'}) \mathcal{T}_{kk'}^{(i)} \otimes T_{iL,jL'} \} + \dots \\ & \dots + \sum_{iL,jL'} \sum_{kk'} \{ (h_{iL,jL'}^{AB} \Gamma_{kk} + h_{iL,jL'}^{CB} \mathcal{S}_{kk}) \mathcal{T}_{kk'}^{(j)} \otimes T_{iL,jL'} \} + \dots \\ & \dots + \sum_{iL,jL'} \sum_{k,k',k'',k'''} M_{k,k',k'',k'''}^{iL,jL'} \mathcal{T}_{k'k''}^{(j)} \otimes \mathcal{T}_{kk'''}^{(i)} \otimes T_{iL,jL'} \end{aligned}$$

with

$$\begin{aligned} E_{k,k'}^{iL} &= \hat{C}_{2L} \Gamma_{k,k'} + \hat{C}_{3L} \mathcal{S}_{k,k'} \\ M_{k,k',k'',k'''}^{iL,jL'} &= h_{iL,jL'}^{AA} \Gamma_{k',k''} \mathcal{S}_{k,k'''} + h_{iL,jL'}^{AC} \Gamma_{k',k''} \mathcal{S}_{k,k'''} + h_{iL,jL'}^{CA} \Gamma_{k',k''} \mathcal{S}_{k,k'''} + h_{iL,jL'}^{CC} \mathcal{S}_{k',k''} \mathcal{S}_{k,k'''} \end{aligned}$$

Once we have identified the augmented space Hamiltonian, the choice of basis states in Hilbert and configuration spaces is exactly similar to the binary case [7]. The Hilbert space basis vector is represented a column vector  $C_m$  with zeros everywhere except at the  $m$ th position. The inner product is defined as

$$\langle m | \odot | n \rangle = C_m^\dagger C_n.$$

In order to represent a basis vector in configuration space we allocate for each site two bits instead of a single bit as in the binary case [7]. The combination of two bits can take values 00, 10 and 11 representing the three possible configurations at the site. The inner product between the basis vectors in configuration space is defined as

$$\langle C'_1, C'_2, \dots, C'_i, \dots | \odot | C_1, C_2, \dots, C_i \rangle = \delta\{C_i, C'_i\}.$$

$C_i$  and  $C'_i$  represent combinations of two bits at the  $i$ th site for two different configurations.

Choosing the starting state of the recursion method as

$$|\xi_1\rangle = |R_i, L\rangle \otimes |\Phi_0\rangle$$

where

$$|\Psi_0\rangle = |C_1^0, C_2^0, \dots, C_i^0, \dots\rangle$$

with  $C_i^0$  indicating the configuration {00} at the site  $i$ , the subsequent states are then generated in the process of recursion as mentioned in section 2.

#### 4. Computational details

For calculating the component projected average density of states for A, B and C components of disordered ternary alloys we have used the augmented space map generated from a real space cluster of 400 atoms and determined eight pairs of recursion coefficients terminated by the herglotz termination scheme of Lucini and Nex [15].

As already mentioned, the basic philosophy of the configuration averaging procedure in augmented space formalism is to expand the Hilbert space to include a disorder space in which configuration fluctuations are described. Hence for a system with  $N$  sites and  $m$  possible realizations of the random variable the augmented space involved  $Nm^N$  basis functions. The standard method for implementing this on a computer would require handling

an impossibility large  $(Nm^N) \times (Nm^N)$  matrix. Working with this large (even though sparse) Hamiltonian within the recursion method becomes a difficult task for real alloy systems with s-p-d orbitals.

Two major advancements were proposed in this direction.

Firstly, the conceptual advantages in the augmented space formalism include, apart from analyticity, translational and rotational invariance automatically built into the augmented space Hamiltonian<sup>†</sup>. This allows us to invoke the idea of utilizing symmetry operations present in the full augmented space in the context of recursion, thus actually working in an invariant subspace of much reduced rank.

The philosophy of utilizing symmetry in the recursion method operationally is as follows.

Basis vectors, defined iteratively in the recursion procedure, carry information on a more and more distant environment of the starting state  $|\xi_0\rangle$ . The vector  $H|\xi_0\rangle$  is the combination of states with which  $|\xi_0\rangle$  interact and the relative contribution of a state  $|\xi_n\rangle$  in  $H|\xi_0\rangle$  is proportional to the strength of interaction between  $|\xi_n\rangle$  and  $|\xi_0\rangle$ . The orbitals sitting at sites which are connected by point group symmetry operations to each other have identical coupling to  $|\xi_0\rangle$ . If  $\mathcal{T}$  is a unitary representation of a symmetry operation, then the states generated by unitary transformations  $\mathcal{T}|\xi_n\rangle$  carry the same information as  $|\xi_n\rangle$ . Hence, it is useful to consider among the states coupled to  $|\xi_0\rangle$  only those belonging to the irreducible part of the full Hilbert space and redefine the Hamiltonian operation so as to reduce the computer storage and time [16].

As discussed earlier a general basis in augmented space is the direct product of the lattice space basis vector and the configuration space basis vector.

$$|\xi\rangle = |R\rangle \otimes \{|\sigma_1, \sigma_2, \dots, \sigma_r\rangle\}.$$

The configuration space basis vector is uniquely specified by the set of points  $\{\sigma_i\}$  at which there are *excitations* and by the type of excitation. By excitations we mean the states describing fluctuations about the average state  $|\nu_0\rangle$ . According to our convention, for the binary case there can be only one type of excitation, characterized by 1, while for the ternary case there are two different types of excitation, characterized by 1 and  $-1$ . The augmented space Hamiltonian commutes with all the symmetry operations of the Hilbert space.

The transformation of basis orbitals under the point group symmetry operation is given by

$$\mathcal{T}\{|R\rangle \otimes \{|\sigma_1, \sigma_2, \dots, \sigma_r\rangle\}\} = \mathcal{T}|R\rangle \otimes \{|\mathcal{T}\sigma_1, \mathcal{T}\sigma_2, \dots, \mathcal{T}\sigma_r\rangle\} = |R'\rangle \otimes \{|\sigma'\rangle\}.$$

Thus the equivalent states corresponding to  $|\xi\rangle$  are obtained by applying symmetry operations independently both to the lattice space and configuration space and picking up only the distinct states.

The redefined Hamiltonian operation with only inequivalent states is given by

$$\langle \xi_I | \tilde{H} | \xi_J \rangle_{mod} = \langle \xi_I | \tilde{H} | \xi_J \rangle \sqrt{W_I / W_J} \quad (7)$$

where  $W_I$  and  $W_J$  are the number of distinct states connected by symmetry operations to  $|\xi_I\rangle$  and  $|\xi_J\rangle$ .

The equation (2) is valid for orbitals having spherical symmetry only. Introduction of orbitals without spherical symmetry introduces another factor of  $\beta_{\xi_i}(L, L')$  determining where the state  $\xi_I$  is a symmetric state with respect to orbitals  $L$  and  $L'$ . The effective irreducible basis, which is a linear combination of the old basis sets, reflects the symmetry

<sup>†</sup> Although the states in the Hilbert space  $\mathcal{H}$  have neither translational nor local lattice group symmetries, because the disorder is homogeneous and isotropic in the bulk, it is easy to see that these symmetries are restored in the full augmented space.

of the orbital itself and it is the symmetry of the orbitals which prohibits the overlap at a particular site. We call these positions symmetry positions with respect to overlapping orbitals. A given site in augmented space is a symmetric site with respect to the orbitals  $L$  and  $L'$  if the real space site  $R$  and the sites  $\{\sigma_i\}$  at which there are excitations satisfy the condition of being symmetric with respect to orbitals  $L$  and  $L'$ .

We have already applied the symmetry reduction scheme for disordered binary alloys [7]. We now apply it to ternary alloys. The only difference between the application of symmetry reduction in binary and ternary alloys is that, in contrast to binary alloys, for ternary alloys one has to distinguish between two different types of excitation (namely 1 and  $-1$ ) and the symmetry operations connect only the states having same type of excitation.

The second point leading to memory reduction and time saving for augmented space recursion is the use of the multi-spin coding technique. Since we store the basis vectors in configuration space in bits, one can utilize the bit manipulation techniques and logical functions predefined in the computer. To make use of the bit manipulation technique for ternary alloys we proceed as follows. As already mentioned we allocate two bits to describe the configuration state of each site. For the possible combinations (00) denotes the reference state 0 (site occupied by the average state), (10) denotes the configuration state 1 while (11) denotes the configuration state  $-1$ . In an  $M$ -bit machine, each  $M$ -bit word can represent up to  $(M - 1)$  terms as a sequence of 0s and 1s. To store a configuration of a ternary alloy with  $N$  lattice points the number of words required are  $2N/(M - 1)$  (as we need two bits to define the configuration of a given lattice point). We define two sets of words denoted by  $\{B_1\}$  and  $\{B_2\}$ . Each word is characterized by the number of non-zeros (the *cardinality*:  $C$ ) and the positions where these occur (the *cardinality sequence*:  $\{S_C\}$ ). The configuration corresponding to the  $i$ th site is stored in the  $m$ th position of the  $n$ th  $B_1$  and  $B_2$  types of word.

Let  $\mathcal{L}_1$  and  $\mathcal{L}_2$  be the bit types 0 or 1 at the  $m$ th position of the  $n$ th  $B_1$  and  $B_2$  words respectively i.e.

$$\mathcal{L}_1 = \phi_B(m)B_1[C, \{S_C\}]$$

and

$$\mathcal{L}_2 = \phi_B(m)B_2[C, \{S_C\}]$$

where  $\phi_B$  is the logical function IBITS that returns the bit type at a particular position of a word. Then the configuration at the  $i$ th site is given by  $\mathcal{L} = \mathcal{L}_1 - 2\mathcal{L}_2$

$$\text{for } \mathcal{L}_1 = 0 \ \mathcal{L}_2 = 0 \Rightarrow \mathcal{L} = 0$$

$$\text{for } \mathcal{L}_1 = 1 \ \mathcal{L}_2 = 0 \Rightarrow \mathcal{L} = 1$$

$$\text{for } \mathcal{L}_1 = 0 \ \mathcal{L}_2 = 1 \Rightarrow \mathcal{L} = -1$$

we exclude the case  $\mathcal{L}_1 = 0$  and  $\mathcal{L}_2 = 1$ .

The Hamiltonian operation in configuration space which is essentially changing the configuration states from 0 to 1 or  $-1$ , 1 to 0 or  $-1$  and  $-1$  to 0 or 1 can then be written in compact form as the following two sets of operations:

Set 1:

$$B'_1[C', \{S_{C'}\}] = (1 - \mathcal{L}_1)\phi_S(m)B_1[C, \{S_C\}] + \mathcal{L}_1\phi_C(m)B_1[C, \{S_C\}]$$

$$B'_2[C', \{S_{C'}\}] = (1 - \mathcal{L}_2)\phi_S(m)B_2[C, \{S_C\}] + \mathcal{L}_2\phi_C(m)B_2[C, \{S_C\}]$$

$\{0 \rightarrow 1; 1 \rightarrow 0; -1 \rightarrow 0\}$ .



Set 2:

$$B'_1[C', \{S_{C'}\}] = (1 - \mathcal{L}_1)\phi_S(m)B_1[C, \{S_C\}] + \mathcal{L}_1\phi_C(m)B_1[C, \{S_C\}]$$

$$B'_2[C', \{S_{C'}\}] = (1 - \mathcal{L}_2)\phi_S(m)B_2[C, \{S_C\}] + \mathcal{L}_2\phi_C(m)B_1[C, \{S_C\}]$$

$\{0 \rightarrow -1; 1 \rightarrow -1; -1 \rightarrow 1\}$ .

The  $\phi_S$  and  $\phi_C$  are the logical functions IBSET and IBCLR (predefined in Fortran) which correspond to operations of setting bit type equal to 1 and 0 respectively.

## 5. Results and discussion

We have applied the augmented space recursion within the framework of TB-LMTO for disordered ternary alloys Cu–Ni–Zn and Ag–Pd–Rh. In both these alloys the constituents are from the same row of the periodic table and are neighbours. This results in very little charge transfer effect between the constituents. We take into account the effect of charge transfer by taking advantage of the flexibility of Wigner–Seitz radii in TB-LMTO, a fact discussed in great detail elsewhere [17]. Furthermore, any theory on ternary alloys should correctly reduce to the corresponding binary alloy limit for the concentration of one component tending to zero. Some of the binary subsystems of the ternary systems Cu–Ni–Zn and Ag–Pd–Rh have been studied previously with the TB-LMTO-ASR method (Cu–Zn [18], Cu–Ni [14], Ag–Pd [7], Pd–Rh [19]). In figures 1 and 2 we present the density of states for Cu–Ni–Zn alloys and Ag–Pd–Rh alloys for the 40–30–30 concentrations. In both cases we observe the effect of dominant diagonal disorder effect and split bands.

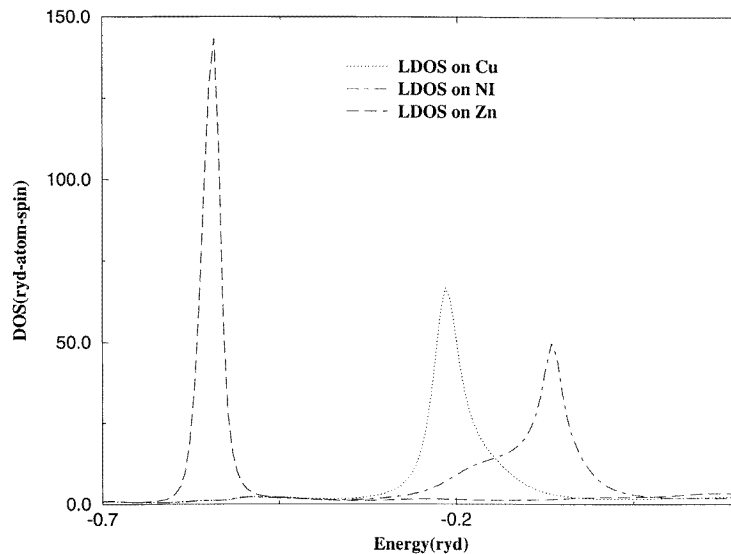


**Figure 1.** The local density of states in states  $\text{Ryd}^{-1}/\text{atom}$  on Cu (dotted), Ni (dash-dotted) and Zn (long-dashed) sites for  $\text{Cu}_{40}\text{Ni}_{30}\text{Zn}_{30}$  alloys. Energy is measured from the Fermi energy in Rydbergs.

As a special case for comparison of our approach with both the earlier theoretical CPA, as well as experimental results, we consider the case of the ternary system Fe–Cu–Ag. These compounds are artificially prepared and do not exist in the equilibrium solid state.

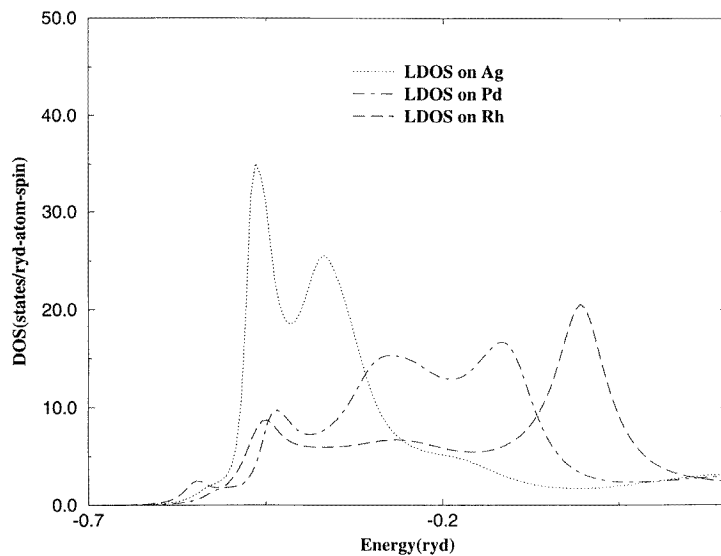


**Figure 2.** The local density of states in states  $\text{Ryd}^{-1}/(\text{atom spin})$  on Ag (dotted), Pd (dash-dotted) and Rh (long-dashed) sites for  $\text{Ag}_{40}\text{Pd}_{30}\text{Rh}_{30}$  alloys. Energy is measured from the Fermi energy in Rydbergs.

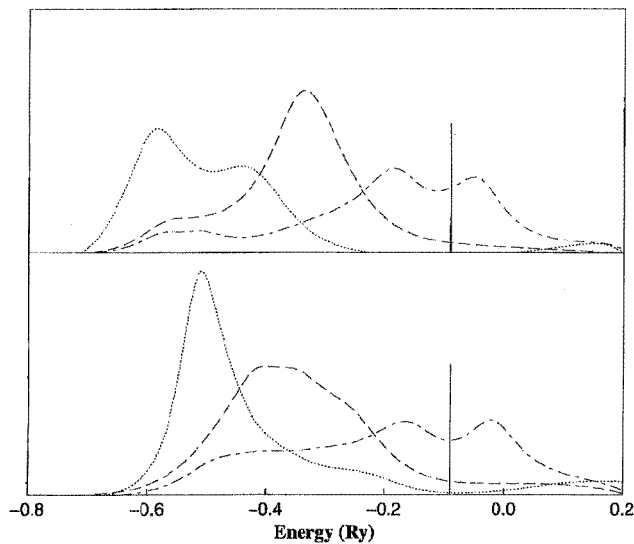
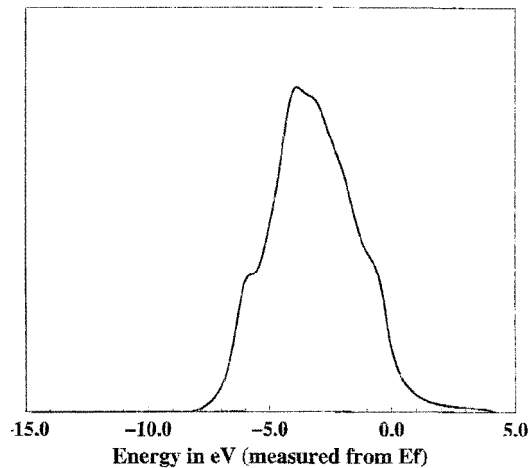
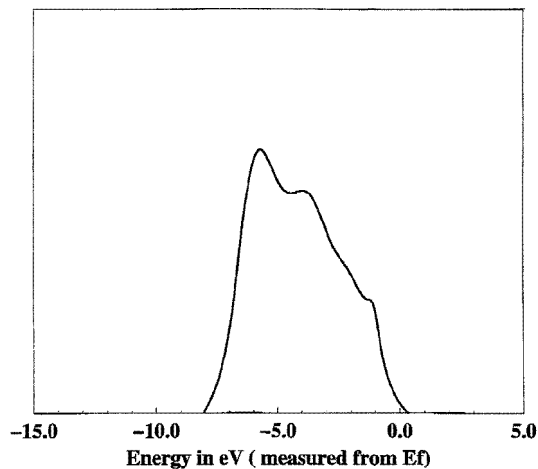


**Figure 3.** The local densities of states in states  $\text{Ryd}^{-1}/\text{atom}$  on Ag (dotted), Cu (dashed) and Fe (dash-dotted) sites for (bottom)  $\text{Fe}_{44}\text{Cu}_{46}\text{Ag}_{10}$  and (top)  $\text{Fe}_{38}\text{Cu}_{09}\text{Ag}_{53}$ .

They are metastable and homogeneous and are produced by sputtering techniques over a large composition range [20–22]. In particular, two alloys  $\text{Fe}_{38}\text{Cu}_{09}\text{Ag}_{53}$  and  $\text{Fe}_{44}\text{Cu}_{46}\text{Ag}_{10}$  are formed in the fcc phase [22]. Kudrnovský *et al* have studied the density of states and XPS spectra of these alloys using the ternary generalization of the TB-LMTO-CPA [3]. This is an ideal result against which to compare our TB-LMTO-ASR, since both methods have



(a)



(b)

**Figure 4.** XPS spectra for the (a) Cu-rich and (b) Ag-rich alloys. Both spectra have been normalized to a common maximum intensity of 1 to facilitate comparison.

the TB-LMTO as their basis and thus the associated approximations and errors, in the basis at least, are similar. Hüfner *et al* [5] noted that for Cu-rich CuNi and Ag-rich PdAg alloys the CPA does not work well in the minority bands. This was noted and emphasized in many earlier works (see references in [7]). The energy separations between the Cu 3d, or Ag 4d, and the Fe 3d bands are in fact larger than separations in CuNi and PdAg. It should be interesting to go beyond the CPA. This point has been noted by Ushida *et al* [22]. The generalization of our TB-LMTO-ASR which is based on the LDA to include the effects of magnetic constituents is straightforward, with the LSDA replacing the LDA. As a starting point of our LSDA iterations in the ASR, we have first run the self-consistent CPA codes, choosing the variable atomic spheres around the three constituents in such a way that the volume is conserved, each sphere is almost neutral and the sphere overlap is less than 15%. This procedure was suggested earlier by Drchal *et al* [23] in order to avoid the controversies

related to the definition of the Madelung energy in random alloys. It must be noted that the method is ingenious, but there is no *a priori* guarantee that we will manage to find such a triplet of sphere radii satisfying all three conditions mentioned above. With this input, a few ASR self-consistently iterations lead to convergence.

Figure 3 shows the partial densities of states of the two alloy systems on Fe, Ag and Cu atoms. The results agree in detail with the corresponding results in the CPA work [3]. Minor differences are noticeable in the Ag and Fe partial densities. The structures are similar but relative weights for Ag in the Ag-rich alloy and Fe in both alloys are slightly different.

The XPS photocurrent is given by

$$I(E + \omega) = \sum_Q \sum_L \sum_\sigma x_Q M_{L\sigma}^Q(E + \omega) n_{L\sigma}^Q \Theta(E_F - E).$$

Here,  $Q = \text{Ag, Cu or Fe}$ ;  $\omega$  is the incident photon energy (for the  $K\alpha$  line of Al this is 109.3 Ryd (1486.6 eV)).  $M_{L\sigma}^Q(E + \omega)$  are the photoionization cross-sections for the constituents. These are dominated by the d contributions and we approximate these as in the CPA work by their atomic counterparts  $M_d^Q(\omega)$ . Given the incident photon energy, we may locate these values in spectroscopic tables [23, 4]:

$$M_d^{Fe} : M_d^{Cu} : M_d^{Ag} = 1 : \frac{5}{2} : \frac{9}{2}.$$

Finally, as in the earlier work, we broaden the spectra with a Lorentzian of half-width 0.03 Ryd.

Figure 4 shows the XPS spectra, which agree excellently with the CPA as well as with experiment. Table 1 clarifies this agreement. Perhaps the ASR does fractionally better, but given the approximations in both the theory and experiment, perhaps one cannot make a strong statement.

**Table 1.** Comparison between experimental data, TB-LMTO-CPA and TB-LMTO-ASR on XPS spectra on FeCuAg alloys. Energies are measured in eV from the Fermi energy.

Peak (numbered from left)	Expt	TB-LMTO-CPA	TB-LMTO-ASR
I	-6.0	-6.25	-6.0
II	-3.0	-3.4	-2.9
III	-0.5	-0.62	-0.62

## Acknowledgment

AM would like to thank the Department of Science and Technology, Government of India for financial help through their project.

## References

- [1] Kudrnovský J, Drchal V and Mašek J 1987 *Phys. Rev. B* **35** 2487
- [2] Kudrnovský J, Drchal V, Šob M, Christensen N E and Andersen O K 1989 *Phys. Rev. B* **40** 10 029
- [3] Kudrnovský J, Bose S K and Andersen O K 1990 *J. Phys.: Condens. Matter* **2** L6847
- [4] Kudrnovský J, Bose S K and Andersen O K 1990 *J. Phys. Soc. Japan* **59** 4511–19
- [5] Hüfner S, Wertheim G K and Wernick J H 1973 *Phys. Rev. B* **8** 4511
- [6] Mookerjee A 1973 *J. Phys. C: Solid State Phys.* **6** 1340
- [7] Saha T, Dasgupta I and Mookerjee A 1994 *J. Phys.: Condens. Matter* **6** L245

- [8] Haydock R, Heine V and Kelly M J 1972 *J. Phys. C: Solid State Phys.* **5** 2845
- [9] Andersen O K and Jepsen O 1984 *Phys. Rev. Lett.* **53** 2571
- [10] Saha T, Dasgupta I and Mookerjee A 1994 *Phys. Rev. B* **50** 13 267
- [11] Saha T and Mookerjee A 1996 *J. Phys.: Condens. Matter* **8** 2915
- [12] Dasgupta I, Saha T and Mookerjee A 1995 *Phys. Rev. B* **51** 3413
- [13] Thakur P K and Mookerjee A 1988 *Phys. Rev. B* **38** 3798
- [14] Datta A and Mookerjee A 1992 *Int. J. Mod. Phys. B* **6** 3295
- [15] Lucini M U and Nex C M M 1987 *J. Phys. C: Solid State Phys.* **20** 3125
- [16] Gallagher J 1978 *PhD Thesis* University of Cambridge
- [17] See articles, Andersen O K, Kumar V and Mookerjee A (ed) 1995 *Electronic Structure of Metals and Alloys* (Singapore: World Scientific)
- [18] Saha T, Dasgupta I and Mookerjee A J 1996 *J. Phys.: Condens. Matter* **8** 1979
- [19] Saha T and Mookerjee A 1996 *J. Phys.: Condens. Matter* **8** 2915
- [20] Sumiyama K, Yoshitake T and Nakamura Y 1984 *J. Phys. Soc. Japan* **53** 3160
- [21] Chien C L, Liou S H, Kofalt D, Yu Wu, Egami T and McGuire T R 1986 *Phys. Rev. B* **33** 3247
- [22] Ushida M, Tanaka K, Sumiyama K and Nakamura Y 1989 *J. Phys. Soc. Japan* **58** 1725
- [23] Drchal V, Kudrnovský J and Weinberger P 1994 *Phys. Rev. B* **50** 7903